Capacitive and inductive effects in multi-Josephson junction model in high T_c superconductors

Hideki Matsumoto [a,1], Shoichi Sakamoto [b], Satoshi Katoh [b]

[a] *Institute of Physics, University of Tsukuba, Ibaraki 305-8571, Japan*

[b] *Department of Applied Physics, Seikei University, Musashino 180-8633, Japan*

Abstract

I-V characteristics of high T_c superconductors, such as $Bi_2Sr_2CaCu_2O_8$, are well described by use of the multi-Josephson junction model. I-V characteristics are investigated, including both capacitive and inductive effects. It is shown that both effects are equally important to get systematic changes of I-V characteristics from short junctions to long ones, and their dependence on the applied magnetic field.

Key words: multi-Josephson junction; I-V characteristics; high T_c superconductor;

1. Introduction

I-V characteristics of the high T_c superconductor $Bi_2Sr_2Ca_1C_2O_8$ (BSCCO) shows a strong hysteresis, producing multi-branches [1]. As mechanisms of the inter-layer coupling, there are the capacitive effect[2] and inductive effect. It has been argued that the inductive effect is much important than the capacitive one in high T_c superconductors[3], since scaled parameters are much larger for the former effect. In this paper, we include both capacitive and inductive effects to investigate I-V characteristics and shows that the two mechanism give different effects in behavior of I-V curves and equally important.

2. Formulation

Let us consider a multi-Josephson junction stacked with N-layers along z-axis and having a length L along x-axis with a magnetic filed H being applied along y-axis uniformly.

Taking into account of the layered structure, we discretize the z-direction of physical quantities, and represents them either on the superconducting or normal layers. Namely, we consider the current $\mathbf{j} = (j_s, 0, j_n)$, the electric field $\mathbf{E} = (0, 0, E_n)$, the magnetic induction field $\mathbf{B} = (0, B_n, 0)$, as indicated in FIg.1, with the subscript "s" and "n" indicating quantities on superconducting and normal layers, respectively. On the superconducting layer, we neglect the electric field, that is, $(\nabla \times \mathbf{B})_s = \frac{4\pi}{c}\mathbf{j}_s$. The expression of the current j_n is given by $j_n(\ell) = \sigma E_n(\ell) + j_c \sin(\phi(\ell))$, where $\phi(\ell)$ is the gauge invariant phase difference at the ℓth junc-

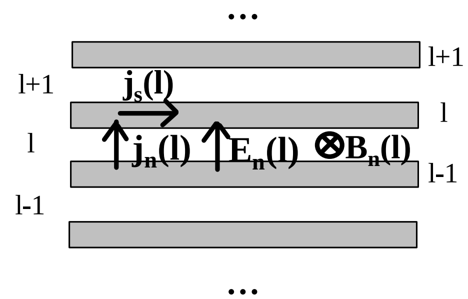

Fig. 1. Multi-Josephson junction

[1] Corresponding author, E-mail:matumoto@cm.ph.tsukuba.ac.jp

tion. The boundary condition is taken, on the side of the junctions, as $B_n(\pm L/2, \ell) = H \pm JL/2$ with JL being the applied current. By taking $\phi = \phi_0 + \phi_b$ with $\phi_0 = Hx + \frac{1}{2}Jx^2$ and $B_n = b_0 + b_n$ with $b_0 = H + Jx$ and from the Maxwell equations and relations between space-time variation of ϕ and electromagnetic field[2], we have the following coupled differential equation to determine the electromagnetic properties of the system

$$\frac{1}{\omega_p}\frac{\partial}{\partial t}\phi_b(\ell) = (1 - \alpha\Delta_z^2)\frac{E_n(\ell)}{E_p} \ , \tag{1}$$

$$\frac{1}{\omega_p}\frac{\partial}{\partial t}\frac{E_n(\ell)}{E_p} = \frac{J}{j_c} + \gamma\left(\lambda_a \nabla_x \frac{b_n(\ell)}{B_a}\right)_z - \left(\beta\frac{E_n(\ell)}{E_p} + \sin(\phi_b(\ell) + \phi_0)\right) , \tag{2}$$

$$\gamma\frac{B_n(\ell)}{B_a} = \gamma(1 - \alpha_s\Delta_z^2)^{-1}\lambda_a\nabla_x\phi_b(\ell) \ . \tag{3}$$

where $\Delta_z^2 f$ indicates $f(\ell+1) - 2f(\ell) + f(\ell-1)$, and the notations are those used in ref.[4], and $B_a = \frac{\hbar c}{2e}\frac{1}{D\lambda_a}$, $\gamma = \frac{\lambda_p^2}{\lambda_a^2}$, $\alpha_s = \frac{\lambda^2}{sD}$.

3. Numerical results and Conclusion

Numerical simulation is performed by use of the fourth order Runge-Kutta method for time-evolution. For $Bi_2Sr_2Ca_1Cu_2O_8$, we choose $\lambda_p = 12.5 \times 10^5 \mathring{A}$ and $\lambda_a = 2.5 \times 10^3 \mathring{A}$. Other parameters are chosen as those used in ref.[4]. We have $\alpha = 1.0$, $\beta = 0.2$, $\gamma = 2.5 \times 10^5$, $\alpha_s = 1.736 \times 10^5$.

The length dependence of I-V characteristic is calculated in the case of $N = 5$ and $H = 0.0$. Fig.2 is for $\alpha = 0.0$ and Fig. 3 is for $\alpha = 1.0$. The length L is changed as $L/\lambda_a = 0.5, 1.0, 5.0, 10.0$. The current density J/j_c is increased up to 2.0 and decreased to zero. Branch structures are observed in both cases. However, in the $\alpha = 0$ case, there appears no voltage jump in the current-increasing process except the last big jump. In Fig. 3, long branches with large jumps and short branches with small jumps are observed. The large jumps are related to change in the number of rotating phase modes in layered junctions, as was discussed in ref.[4]. The small branches are originated from the spatial dependence of phase-differences induced by the inductive effect.

We only report here that, when the magnetic field is applied and increased, both cases with $\alpha = 0$ and 1 show a similar behavior of I-V characteristics.

From the numerical analysis of the present paper, we see that both capacitive and inductive effects are

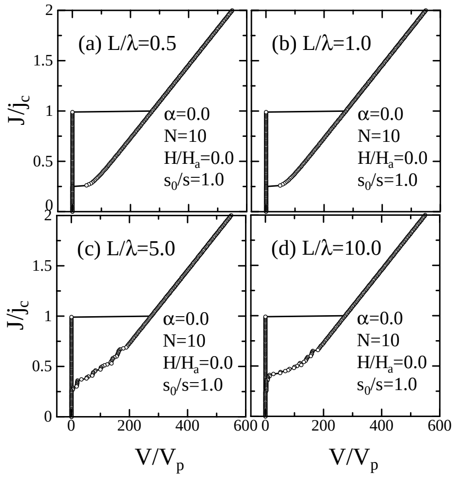

Fig. 2. L-dependence of I-V characteristics for $\alpha = 0.0$

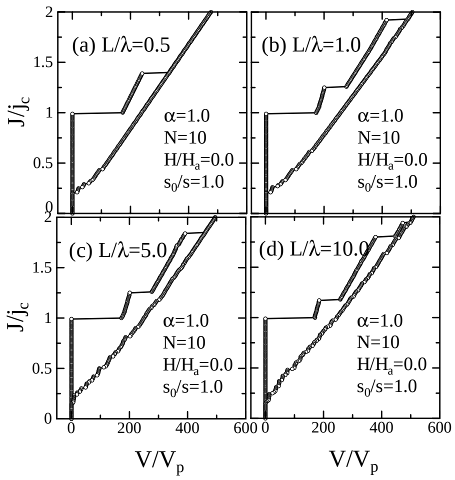

Fig. 3. L-dependence of I-V characteristics for $\alpha = 1.0$

necessary to describe the I-V characteristics of multi-Josephson junctions. The inductive effect works to move phase differences of layers together, while the capacitive effect controls easier layers to enter rotating phase modes. Because of this two mechanism, the I-V characteristics shows branch structures which are grouped by sub-branch structure of small jumps. This feature is the one observed in I-V characteristics of $Bi_2Sr_2CaCu_2O_4$.

References

[1] R. Kleiner, et.al., Phys. Rev. Lett. **68** (1992) 2394.

[2] T. Koyama and M. Tachiki, Phys. Rev. B**54** (1996) 16183.

[3] R. Kleiner, et.al., Phys. Rev. B**62** (2000) 4086.

[4] H. Matsumoto, et.al., Phys. Rev. B 60, 3666 (1999).